NOS3 regulates angiogenic potential of human induced pluripotent stem cell-derived endothelial cells

Anne M. Kong [a], Zulhusni A. Idris [a,b], Daniel Urrutia-Cabrera [c,d], Jarmon G. Lees [a,c], Ren Jie Phang [a], Geraldine M. Mitchell [a,c,e], Raymond C.B. Wong [c,d], Shiang Y. Lim [a,c,f,g,*]

[a] O'Brien Institute Department, St Vincent's Institute of Medical Research, VIC, Australia
[b] School of Engineering, University of Melbourne, VIC, Australia
[c] Departments of Surgery, Ophthalmology and Medicine, University of Melbourne, VIC, Australia
[d] Centre for Eye Research Australia, Royal Victorian Eye and Ear Hospital, East Melbourne, Victoria, Australia
[e] Faculty of Health Sciences, Australian Catholic University, VIC, Australia
[f] Drug Discovery Biology, Faculty of Pharmacy and Pharmaceutical Sciences, Victoria, Monash University, Australia
[g] National Heart Research Institute Singapore, National Heart Centre, Singapore

ARTICLE INFO

ABSTRACT

Incorporation of blood capillaries in engineered tissues and their functional connection to host blood vessels is essential for success in engineering vascularized tissues, a process which involves spatial patterning of endothelial cells (ECs) to form functional and integrated vascular networks. Different types of ECs have been employed for vascular network formation and each source offers advantages and disadvantages. While ECs derived from induced pluripotent stem cells (iPSC-ECs) offer advantages over primary ECs in that they can be generated in large quantities for autologous applications, their suitability for disease modelling and cell replacement therapies is not well-explored. The present study compares the angiogenic capacity of iPSC-ECs and primary ECs (cardiac microvascular ECs and lymphatic microvascular ECs) using an *in vitro* tubulogenesis assay, revealing comparable performance in forming a pseudo-capillary network on Matrigel. Analysis of genes encoding angiogenic factors (*VEGFA*, *VEGFC*, *VEGFD* and *ANG*), endothelial cell markers (*PECAM1*, *PCDH12* and *NOS3*) and proliferation markers (*AURKB* and *MKI67*) indicates a significant positive correlation between *NOS3* mRNA expression levels and various tubulogenic parameters. Further experimentation using a CRISPR activation system demonstrates a positive impact of *NOS3* on tubulogenic activity of ECs, suggesting that iPSC-ECs can be enhanced with endogenous *NOS3* activation. Collectively, these findings highlight the potential of iPSC-ECs in generating vascularized tissues and advancing therapeutic vascularization.

1. Introduction

Angiogenesis is a vital process for normal tissue development to ensure sufficient mass transport of nutrients and oxygen to cells, and to overcome diffusion limitations (the oxygen diffusion limit is 150–200 µm [1]). A major issue in the field of tissue engineering is the inability to grow tissues to a size appropriate for therapeutic use. This is mainly due to a lack of a functional and perfusable vascular network to ensure the long-term survival and function of engineered tissues [2–5]. Therefore, achieving consistently successful vascularization of tissues is one of the key factors that will contribute to the major advancement in tissue engineering, allowing larger tissues to be produced with greater therapeutic potential.

Engineering vascularized tissues requires optimal interaction and integration of appropriate cell types within a scaffold in the presence of regulatory signals [6,7]. This study investigated tubulogenesis, and compared different sources of endothelial cells (ECs) *in vitro*, where the ability of ECs to undergo self-assembly into capillary-like structures on a hydrogel was evaluated. Four EC populations from different sources were assayed, two primary EC sources and ECs derived from two different human induced pluripotent stem cell (iPSC) lines. While primary microvascular endothelial cells are an ideal mature cell source for tissue vascularization, these primary cells are typically only available in limited quantities and insufficient for extensive vascularization [8].

Advances in cellular reprogramming has led to the use of iPSCs as an alternative renewable, robust source of autologous ECs for therapeutic vascularization and tissue engineering. iPSCs are generated from individual somatic cells, have an indefinite proliferative capacity and the capability to differentiate into various functional cell types, including ECs [9,10]. Although we and others have demonstrated that ECs derived from iPSCs (iPSC-ECs) can be assembled into a capillary network *in vitro* and inosculate to host capillaries when transplanted *in vivo* [9,10], a recent study has shown that capillary network formation by iPSC-ECs was 5-fold lower when compared to human umbilical vein endothelial cells (HUVEC) [11]. This indicates that differences in the angiogenic potential of iPSC-ECs must be better understood. Here, we performed a side-by-side comparison of the tubulogenic activity and gene expression of iPSC-ECs and primary ECs. We subsequently evaluated the pro-angiogenic role of *NOS3* using a CRISPR activation system to induce endogenous *NOS3* expression in iPSC-ECs.

2. Materials and methods

2.1. Endothelial cell culture

Primary human cardiac microvascular endothelial cells (HMEC-C) and human lymphatic micovascular endothelial cells (HLEC) were purchased from Lonza (MD, USA) and Cascade Biologics (OR, USA), respectively. ECs were generated from human iPSC lines, CERA007c6 (CERA, [12]) and PB001-tdTomato (GT-TT [13,14]) using a protocol adapted from Patsch et al., 2015 [15]. Briefly, undifferentiated iPSCs were dissociated into single cells with TrypLE (Thermo Fisher Scientific, MA, USA) and seeded onto 6-well plate pre-coated with Matrigel hESC-qualified Matrix (Corning, MA, USA) at 100,000 cells/cm^2 in TeSR-E8 medium supplemented with 10 μM Y-27632 (Tocris Bioscience, Bristol, UK) for 24 h. At day 0, medium was replaced with DMEM/F12 GlutaMAX medium (Thermo Fisher Scientific) containing N-2 supplement (1X, Thermo Fisher Scientific), B27 supplement (1X, Thermo Fisher Scientific), 8 μM CHIR99021 (Cayman Chemical, MI, USA) and 25 ng/mL BMP4 (Peprotech, NJ, USA) for 3 days. At day 3, medium was replaced with StemPro-34 SFM complete medium (Thermo Fisher Scientific) supplemented with 200 ng/mL VEGF$_{165}$ (Peprotech) and 2 μM forskolin (Sigma-Aldrich, MO, USA) for 3 days. At day 6, CD31$^+$ cells were labeled with CD31 FITC-conjugated antibody (mouse anti-human IgG; BD Pharmingen, CA, USA), sorted using a Flow cytometer and sorter (Influx, BD Biosciences, NSW, Australia) and expanded in cell culture flasks pre-coated with 10 μg/mL of human fibronectin (Merck Millipore, MA, USA) in EGM-2MV medium (Lonza, MD, USA) supplemented with 50 ng/mL VEGF$_{165}$ [9]. Human iPSC derived endothelial cells remain positive for endothelial cell markers after 4 population doublings, with 79.7 ± 0.3 % CD31$^+$ cells (n = 3 technical replicates) assessed with flow cytometry, and continued to express CD31 and VE-cadherin (Supplementary Fig. 1).

All ECs were cultured in EGM-2MV (Lonza) containing 50 ng/ml VEGF$_{165}$ in flasks pre-coated with human fibronectin. HMEC-C and HLEC were used in all assays at passage 5–6, while iPSC-derived endothelial cells were used at passage 2–3.

2.2. sgRNA design and expression cassette preparation

Short oligonucleotide sgRNA expression cassettes (500 bp) were designed using the Synergistic Activation Mediator (SAM) sgRNA design tool (http://sam.genome-engineering.org/database/) for human genes. Each sgRNA expression cassette contains an upstream U6 promoter, sgRNA sequence (sgRNA1: 5′-AGGATGACTCAGGTCAGAGC-3′; sgRNA2: 5′-TGACCAGTGGTGACTCAGTT-3′) and sgRNA scaffold with a stem extension and stem loop, and were synthesized as gBLOCK gene fragments (Integrated DNA Technologies, IA, USA) as previously described in Ref. [16].

The sgRNA expression cassettes were amplified with a cloning-free

approach using PCR with the following primers:

Sense (5′) primer: 5′-TGAGTATTACGGCATGTGAGGGC-3′
Antisense (3′) primer: 5′-TCAATGTATCTTATCATGTCTGCTCGA-3′

PCR of sgRNAs was undertaken using KOD Hot Start DNA polymerase kit (Merck Millipore, MA, USA). A PCR master mix containing 1x buffer, 1.5 mM MgSO$_4$, 0.2 mM dNTPs, 0.3 μM sense primer, 0.3 μM sense primer, 0.2 ng/μL gBlock sgRNA and 20 mU/μL, was placed in a Veriti™ 96-Well Thermal Cycler (Applied Biosystems) and subjected to the following thermal profile: 95 °C for 2 min (polymerase activation, step 1), 95 °C for 20 s (denaturing, step 2), 66 °C for 10 s (annealing, step 3) and 70 °C for 8 s (extension, step 4). Steps 2–4 were repeated for a total of 30 cycles, followed by 70 °C for 5 min (final extension, step 5) to ensure that any remaining single-stranded DNA was fully elongated. The samples were stored at 4 °C in the short-term to maintain PCR product integrity.

For DNA purification, 10 μL of 6x TrackIt™ Cyan/Yellow loading buffer (Thermo Fisher Scientific) was added to each PCR product and loaded into separate wells of the 2 % agarose gel, containing 5 μL of 20,000X RedSafe™ nucleic acid staining solution (Intron Biotechnology, South Korea), to separate the PCR amplicons using a horizontal gel electrophoresis system (Wealtec, NV, USA) run at 70 mV for 45 min. A 1 Kb Plus DNA ladder (Thermo Fisher Scientific) was included to confirm the size of DNA fragments. Gels were then placed on a UV illuminator and bands excised with a sterile scalpel blade. The weight of excised gel bands was determined, and DNA purification was performed according to the Wizard® Gel and PCR Clean-Up System (Promega, WI, USA) for a final elution volume of 50 μL. Amplified sgRNA expression cassettes were analyzed for DNA concentration using the NanoDrop™ 1000 spectrophotometer (Thermo Fisher Scientific). Samples were then stored at −20 °C until use.

2.3. NOS3 overexpression with CRISPR activation

ECs derived from CERA007c6 iPSCs were plated onto a fibronectin-coated 24-well plate at 3×10^4 cells/well and transfected with (625 ng) dSpCas9-VPR plasmid along with (120 ng) sgRNAs targeting *NOS3* using the Lipofectamine CRISPRMax reagent (Thermo Fisher Scientific) overnight. A dSpCas9-VPR plasmid alone transfection condition was used as a negative control. Cells were harvested for RT-qPCR and tubulogenesis assay at 2 days post-transfection.

2.4. In vitro tubulogenesis assay

Pre-chilled 96-well microplates were coated with 50 μL per well of Growth Factor Reduced Matrigel and incubated at 37 °C for 30 min to solidify. ECs were detached using TrypLE, washed once with PBS (Sigma-Aldrich) and re-suspended in serum-free basal medium, EBM-2 (Lonza, MD, USA), and plated at 1.5×10^4 cells per well. ECs were incubated at 37 °C and the formation of the pseudo-capillary networks was examined microscopically at 2, 4, 6 and 24 h. Images at 4× magnification were acquired with an inverted microscope (Olympus IX-71 microscope) and different angiogenic parameters were measured using the Angiogenesis Analyzer plugin in Image J (Fig. 1A) [17]. Analysis was performed by Z.A.I. and J.G.L.

The *in vitro* tubulogenesis assay was also performed using different matrices, including gelatin (from porcine skin, Sigma-Aldrich), fibrin gel and PuraMatrix synthetic peptide hydrogel (BD Biosciences). Gelatin was dissolved in distilled water to final concentration of 1, 3 and 5 % (w/v) and added to a 96-well microplate at 4 °C overnight. To prepare fibrin gel, 50 μL of human fibrinogen (10 mg/mL, Sigma-Aldrich) was mixed with 5 μL of human thrombin (25 U/mL, Sigma-Aldrich) to initiate cross-linking of fibrin in a 96-well microplate at 37 °C for 30 min. To prepare PuraMatrix synthetic peptide hydrogel, 1 % PuraMatrix solution was diluted to 0.25 or 0.5 % with distilled water. 50 μL of PuraMatrix solution was then added to a 96-well microplate and 3x 100 μL of EBM2 basal media was carefully added to the well to gradually neutralize the
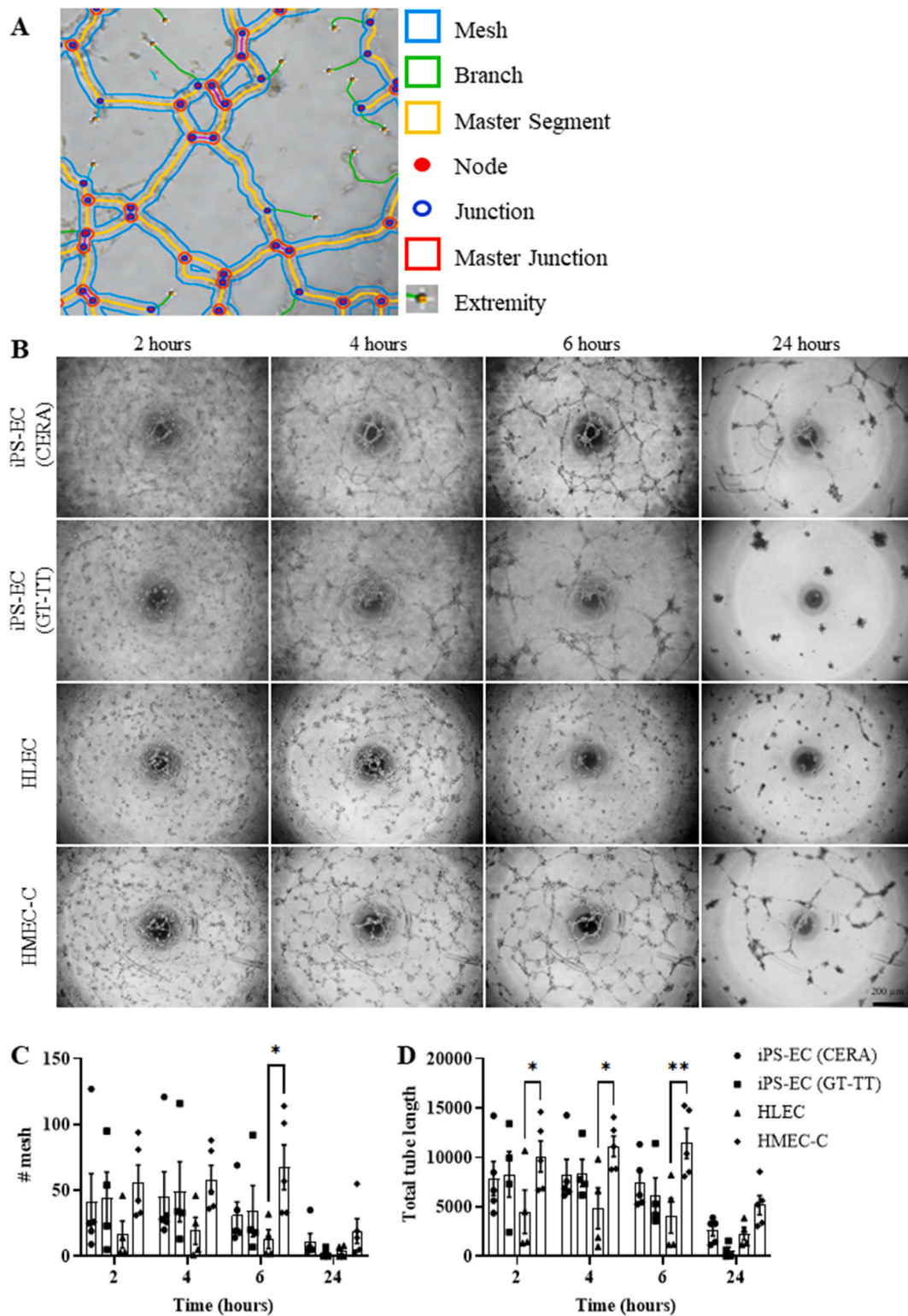
Fig. 1. Endothelial cell capillary tube formation *in vitro* on Matrigel. (A) A representative image of an endothelial cell network on Matrigel with defined parameters. (B) Representative images of vascular network formation of ECs derived from the CERA007c6 iPSC line (iPSC-EC(CERA)), the PB001-tdTomato iPSC line (iPSC-EC(GT-TT)), human lymphatic microvascular endothelial cells (HLEC) and human cardiac microvascular endothelial cells (HMEC-C) on 2D Matrigel at 2, 4, 6 and 24 h. (C-D) Tube formation was assessed by the number of mesh structures (C) and total tube length (D). Data are mean ± SEM from 4 to 5 independent experiments. *P < 0.05, **P < 0.01 by one-way ANOVA with Tukey post hoc test.

matrix pH and allow self-assembly of peptides into nanofibers.

2.5. Reverse transcribed quantitative polymerase chain reaction (RT-qPCR)

RNA was extracted from endothelial cells using TriReagent Solution

(Thermo Fisher Scientific) before RNA precipitation with chloroform and isopropanol (Sigma-Aldrich). cDNA was synthesized using the high-capacity cDNA reverse transcriptase kit with 1 μg of RNA (Applied Biosystems, CA, USA). qPCR was carried out using TaqMan Universal master mix, the Quantstudio 6 Flex PCR system (Thermo Fisher Scientific) and TaqMan gene expression assays (Applied Biosystems) for *GAPDH* (Hs99999905_m1), *VEGFA* (Hs00900054_m1), *VEGFC* (Hs00153458_m1), *VEGFD* (Hs01128659_m1), *ANG* (Hs02379000_s1), *PECAM1* (Hs00169777_m1), *PCDH12* (Hs00170986_m1), *NOS3* (Hs01574659_m1), *AURKB* (Hs00945855_g1) and *MIK67* (Hs01032443_m1). All readings were performed in technical duplicate. The relative quantitation was calculated by applying the comparative CT method (ΔCt), whereby the mRNA expression levels were normalized against the level of the housekeeping gene *GAPDH*.

2.6. Statistics

Data are expressed as mean ± SEM. Statistical analysis was performed using GraphPad Prism software with Student's t-test, one-way ANOVA or two-way ANOVA followed by Tukey's multiple comparison post-hoc analysis where appropriate. Data correlations were evaluated using a Pearson correlation test. $P < 0.05$ was considered statistically significant.

3. Results

3.1. Human iPSC-derived endothelial cells and primary cardiac microvascular endothelial cells have comparable tubulogenic activity

ECs dynamically form pseudo-capillary networks when seeded on a layer of Matrigel with optimal mesh structure occurring by 4–6 h and regressing by 24 h (Fig. 1B). ECs do not form pseudo-capillary networks when seeded onto gelatin (1–5%), fibrin hydrogel or PuraMatrix synthetic peptide hydrogel (Supplementary Fig. S2). ECs derived from two different iPSC lines, CERA and GT-TT, exhibited a similar degree of tubulogenic activity, and were similar to HMEC-C. Interestingly, compared to HMEC-C, HLEC showed reduced tubulogenesis in terms of number of meshes, number of nodes, number of master junctions, number of master segments and total tube length, particularly at 6 h (Fig. 1C and D, Supplementary Fig. S3).
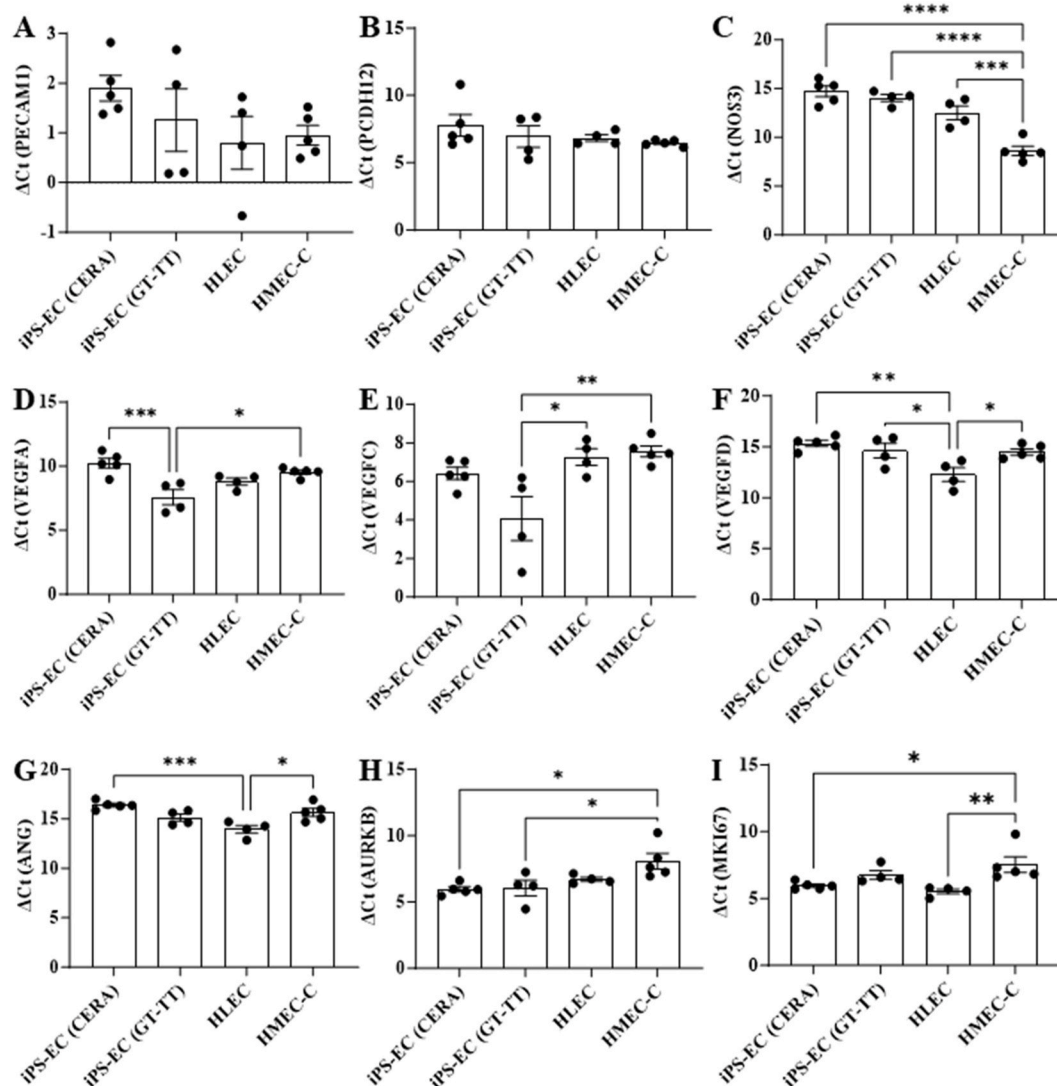

Fig. 2. Gene expression in primary and iPSC-derived endothelial cells. mRNA expression of platelet endothelial cell adhesion molecule/CD31 (*PECAM1*, A), protocadherin-12/VE-cadherin-2 (*PCDH12*, B), endothelial nitric oxide synthase (*NOS3*, C), vascular endothelial growth factor A (*VEGFA*, D), vascular endothelial growth factor C (*VEGFC*, E), vascular endothelial growth factor D (*VEGFD*, F), angiogenin (*ANG*, G), aurora B kinase (*AURKB*, H) and Ki-67 (*MKI67*, I). Data are expressed as mean ± SEM from 4 to 5 independent experiments. *P < 0.05, **P < 0.01, **P < 0.001 by one-way ANOVA with Tukey post hoc test.

3.2. Differential gene expression by different endothelial cells

iPSC-ECs and primary ECs have comparable mRNA expression of endothelial-specific genes, *PECAM1* (CD31) and *PCDH12* (VE-cadherin-2) (Fig. 2A and B). Expression of *NOS3* (nitric oxide synthase 3) gene was significantly higher (lowest ΔCt value) in HMEC-C compared to HLEC and iPSC-ECs (Fig. 2C). Among the four EC sources compared, ECs derived from GT-TT iPSCs have the highest mRNA expression of angiogenic growth factor *VEGFA* and *VEGFC*, while HLEC exhibited the highest mRNA levels of *VEGFD* and *ANG* (angiogenin) (Fig. 2D–G). Expression of cell proliferation genes, *AURKB* and *MKI67*, was lowest in HMEC-C (Fig. 2H and I).

3.3. Expression of NOS3 is positively correlated with tubulogenic activity of endothelial cells

Correlation analysis of gene expression and tubulogenic activity of all four EC sources revealed that most angiogenic parameters (number of master junctions, number of master segments, number of pieces, total tube length, number of branches, total branching length and total master segment length) are significantly and positively correlated with *NOS3* mRNA expression levels (lower ΔCt value indicates higher expression levels resulting in a negative value of Pearson correlation coefficient) (Table 1). The number of extremities is significantly and positively correlated with *PECAM1*, *VEGFD* and *ANG* mRNA expression levels, while the number of pieces and total branching length are significantly and negatively correlated with *AURKB* mRNA expression levels (Table 1). Surprisingly, expression of genes encoding for angiogenic growth factors such as *VEGFA* and *VEGFC* was not correlated to the tubulogenic activity of ECs.

To investigate the regulatory impact of *NOS3* expression on the tubulogenic activity of ECs, endogenous *NOS3* was selectively activated in ECs derived from CERA iPSCs using the CRISPR activation system. Transduction of ECs with a nuclease-null dead SpCas9 coupled with transcription factor activation domains VP64, p65 and Rta (VPR) plasmid, and guided with *NOS3* sgRNA expression cassette, resulted in modest and significant upregulation of *NOS3* mRNA expression levels (Fig. 3A). Activation of endogenous *NOS3* promoted tubulogenic activity of iPSC-ECs, the number of master segments, number of pieces, total

tube length, total master segment length and total branching length were significantly upregulated (Fig. 3B–L).

4. Discussion

Angiogenesis is essential for tissue repair and engineering viable tissue grafts with sufficient thickness (greater than 400 μm) to match the specific tissue being replaced [5,18]. Angiogenesis involves migration and proliferation of ECs to create new tube-like structures and this process can be assayed using an *in vitro* tubulogenesis assay [17,19]. Human iPSC-ECs represent a limitless supply of autologous cells with the potential to address needs unmet by primary ECs, which have limited proliferative potential. In the present study, we showed that the angiogenic capacity of iPSC-ECs was comparable to primary ECs in terms of forming tube-like structures on Matrigel. This finding agrees with a recent study by Fan and colleagues reporting comparable endothelial function in terms of tube formation, the capacity for low-density lipoprotein uptake, and production of vasoconstrictor endothelin-1 and vasodilator nitric oxide, when comparing iPSC-ECs and HMEC-C [20]. Similarly, using a fluid flow dynamic culture system, Lindner et al. showed that iPSC-ECs and HUVECs have a similar capability for glycocalyx formation, which plays an important role in regulating endothelial barrier function [21]. iPSC-ECs and HUVEC have also been demonstrated to exhibit a comparable proteomic profile except for those proteins implicated in mitochondrial metabolism and pro-inflammatory interferon signaling [22]. *In vivo*, iPSC-ECs generated a vascular network comparable to that of HUVEC and human dermal blood ECs in immunodeficient mice [23]. In contrast, a monolayer culture of iPSC-ECs demonstrated lower sensitivity to VEGF-induced changes in transendothelial electrical resistance, a measure of EC barrier function, when compared to HUVEC [24]. Differential responses to barrier-disrupting agents were also reported by Halaidych and colleagues [25] that human dermal blood ECs, but not iPSC-ECs, were responsive to histamine-induced barrier disruption. In terms of inflammatory responses, iPSC-ECs exhibited either a similar [24] or weaker [25] response to the pro-inflammatory cytokine TNFα when compared to HUVECs. When co-cultured with human cardiac fibroblasts, iPSC-ECs formed significantly higher number of junctions and total vessel lengths when compared to primary ECs (human dermal blood ECs and

Table 1

Pearson correlation analysis of different tubulogenesis parameters at 6 h and gene expression compiled from all endothelial cell types (HMEC-C, HLEC, iPSC-EC(CERA) and iPSC-EC(GT-TT)), n = 18 in total.

| Gene expression	Pearson correlation coefficient; P value								
	PECAM1	PCDH12	NOS3	VEGFA	VEGFC	VEGFD	ANG	AURKB	MKI67
# extremities	−0.518; **0.027**[a]	−0.274; 0.271	−0.275; 0.270	−0.070; 0.783	0.136; 0.590	−0.689; **0.002***	−0.525; **0.025***	0.185; 0.463	−0.244; 0.329
# node	0.114; 0.653	−0.039; 0.876	−0.465; 0.052	0.189; 0.452	0.249; 0.319	0.340; 0.167	0.271; 0.276	0.448; 0.062	0.382; 0.118
# master junctions	0.154; 0.542	−0.020; 0.938	−0.534; **0.022**[a]	0.259; 0.299	0.346; 0.159	0.405; 0.095	0.352; 0.152	0.458; 0.056	0.371; 0.130
# master segments	0.164; 0.516	−0.013; 0.960	−0.470; **0.049**[a]	0.232; 0.354	0.303; 0.222	0.395; 0.104	0.326; 0.187	0.450; 0.061	0.382; 0.118
# mesh	0.136; 0.590	−0.007; 0.980	−0.426; 0.078	0.198; 0.432	0.272; 0.276	0.351; 0.153	0.270; 0.278	0.458; 0.056	0.403; 0.098
# pieces	0.076; 0.765	−0.063; 0.805	−0.483; **0.042**[a]	0.174; 0.491	0.272; 0.275	0.276; 0.268	0.215; 0.393	0.471; **0.049**[a]	0.369; 0.132
Total tube Length	0.222; 0.376	−0.018; 0.944	−0.494; **0.037**[a]	0.293; 0.238	0.341; 0.167	0.465; 0.052	0.407; 0.094	0.457; 0.056	0.410; 0.091
# branches	−0.199; 0.429	−0.276; 0.268	−0.550; **0.018**[a]	−0.095; 0.706	0.098; 0.698	−0.075; 0.768	−0.098; 0.697	0.350; 0.154	0.137; 0.587
Total branching length	0.197; 0.433	−0.041; 0.872	−0.515; **0.027**[a]	0.251; 0.315	0.345; 0.161	0.412; 0.089	0.345; 0.161	0.470; **0.049**[a]	0.380; 0.120
Total master segment length	0.222; 0.376	−0.018; 0.944	−0.494; **0.037**[a]	0.293; 0.238	0.341; 0.167	0.465; 0.052	0.407; 0.094	0.457; 0.056	0.410; 0.091
Total branches length	−0.241; 0.336	−0.221; 0.378	−0.328; 0.184	−0.199; 0.428	0.102; 0.686	−0.377; 0.123	−0.381; 0.119	0.093; 0.715	−0.263; 0.292

[a] indicates P < 0.05.
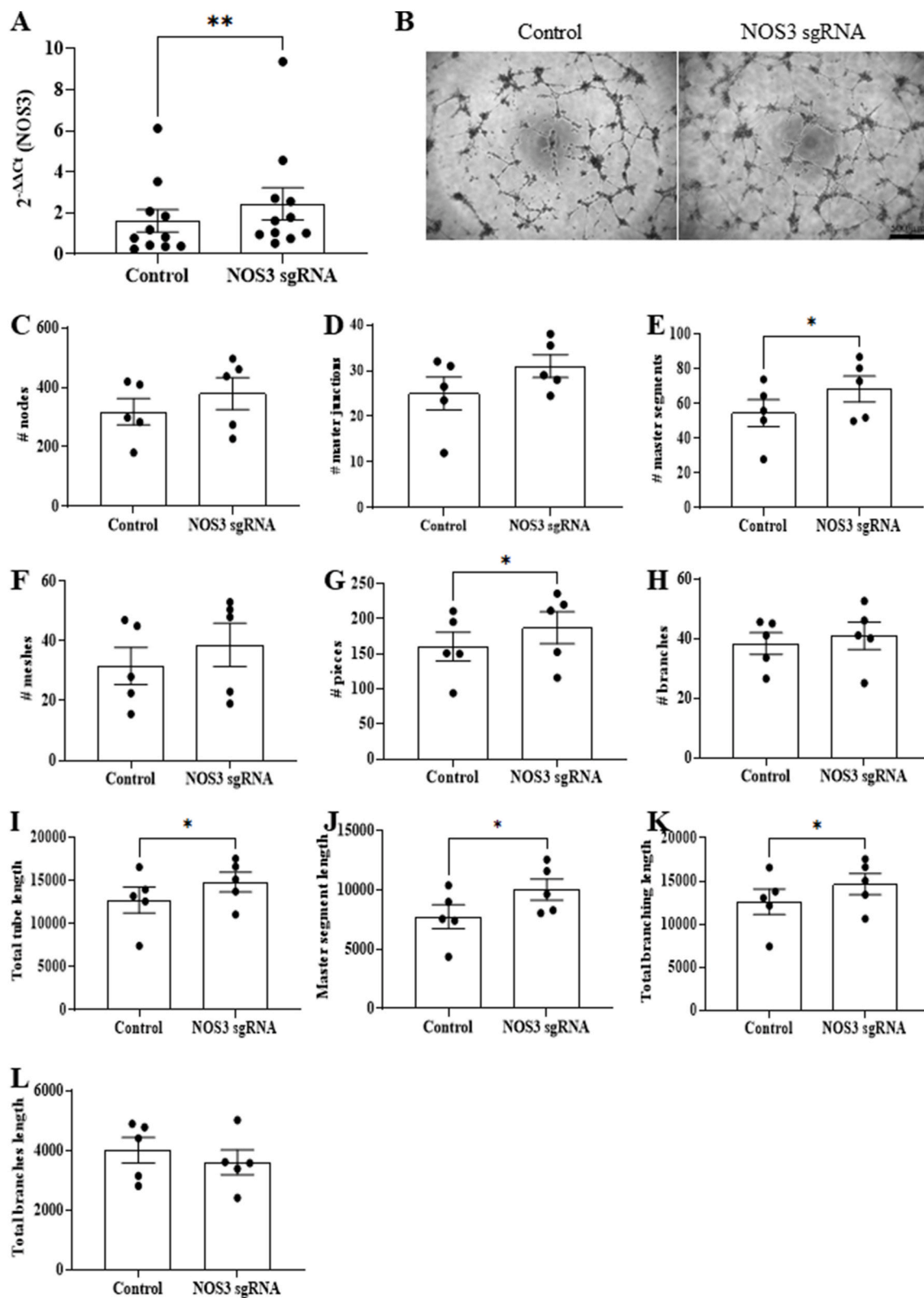
Fig. 3. Endogenous NOS3 gene activation promotes tubulogenic activity of iPSC-derived endothelial cells. (A) RT-qPCR analysis of gene expression for *NOS3* in ECs derived from the CERA007c6 iPSC line (iPSC-EC(CERA)). (B) Representative images of vascular network formation of iPSC-EC(CERA) following *NOS3* gene activation with dSpCas9-VPR at 6 h post-seeding. (C–L) Tube formation was assessed by the number of nodes (C), number of master junctions (D), number of master segments (E), number of meshes (F), number of pieces (G), number of branches (H), total tube length (I), total master segment length (J), total branching length (K) and total branches length (L) at 6 h post-seeding. Data are expressed as mean ± SEM from 4 to 5 independent experiments. *P < 0.05, by paired Student t-test.

HUVECs) [25]. This is in contrast with other studies describing a reduced angiogenic potential in iPSC-ECs when compared to HUVEC in both *in vitro* [11] and *in vivo* [26] settings. Possible explanations for the contrary results could be the different culture conditions and the possibility that different differentiation protocols may generate ECs with different subtypes and properties.

HLEC demonstrated decreased tubulogenic activity in the tubulogenesis assay compared to HMEC-C and hiPSC-ECs. This is likely due to their lymphatic phenotype. Primary lymphatic endothelial cells have been observed to form capillaries more slowly than blood microvascular ECs in 3D culture [27], and are known to form lymphatic capillaries in skin wounds more slowly than blood microvascular ECs [28,29].

Extracellular matrix is an important morphogenic component of tubulogenesis. In the present study, ECs migrated and created pseudo-capillary networks on Matrigel dynamically over the initial 6-h period but showed signs of tubular structure regression by 24 h. The regression of tube-like structures was likely due to the lack of vascular mural cells, such as pericytes and smooth muscle cells, to support stabilization and maturation of tube structures [30]. To address this limitation and to better simulate the physiological process of angiogenesis and vascular function, more sophisticated models that involve co-culture of ECs with vascular mural cells have been developed. For example, 2D coculture of ECs and pericytes derived from human iPSCs [31], haemodynamic coculture of ECs and smooth muscle cells derived from human iPSCs [32], 3D vascular constructs by combining ECs and smooth muscle cells derived from human iPSCs within a supportive matrix [8,33] and 3D vascular organoids differentiated directly from human pluripotent stem cells [34]. The capillary networks of the vascular organoids were found to bear a remarkable resemblance to endogenous blood vessels containing a tubular structure of ECs and pericytes enveloped by a basement membrane [34].

In an attempt to address the inherent batch-to-batch variability and poorly defined composition of Matrigel, we tested other commercially available hydrogels aiming to identify an alternative matrix that can support the tubulogenic activity of ECs. Although gelatin, fibrin gel and PuraMatrix synthetic peptide hydrogel all have defined compositions with minimal batch-to-batch variability, none of these alternative hydrogels were able to support EC tube formation *in vitro*. Alternative matrices, such as laminin and collagen, that can potentially support EC tubulogenic activity should be investigated in future studies.

In the present study, iPSC-ECs exhibited a reduced expression of *NOS3* when compared to HMEC-C. This is consistent with a previous study comparing the gene expression profiles of iPSC-ECs and human aortic ECs [32,35]. Endothelial nitric oxide synthase (eNOS encoded by *NOS3*) plays an important role in maintaining vascular homeostasis and regulating endothelial function through the generation of nitric oxide [36,37]. This potent molecule not only serves as a vasodilator but also demonstrates significant anti-thrombotic and anti-inflammatory effects. Furthermore, nitric oxide is well-recognised for its involvement in angiogenesis and neovascularization [36,38]. The positive correlation between *NOS3* expression and the extent of tubulogenesis in both primary EC and iPSC-ECs underscores the significant role of eNOS in the angiogenic potential of ECs. This association was further supported by the increased tubulogenic activity observed in iPSC-ECs following CRISPR-mediated activation of endogenous *NOS3* expression. This result highlights the angiogenic therapeutic potential of eNOS, as evidenced in patients with pulmonary hypertension receiving endothelial progenitor cells overexpressing eNOS, which led to acute hemodynamic improvement [39]. Similarly, mice with EC-specific eNOS knockout displayed impaired vascular function and dysregulated blood pressure, presenting a hypertensive phenotype that was rescued by reactivation of eNOS in ECs [40].

In conclusion, iPSC-ECs demonstrate angiogenic potential similar to primary ECs, offering a scalable and autologous source for tissue repair. Furthermore, activation of endogenous *NOS3* can enhance the angiogenic potential of iPSC-ECs. These findings advance our understanding of the angiogenic capacity of iPSC-ECs, which is necessary for their increased adoption as therapies, in pharmacological studies, and in toxicological testing.

CRediT authorship contribution statement

Anne M. Kong: Writing – review & editing, Supervision, Methodology, Investigation, Formal analysis, Data curation. **Zulhusni A. Idris:** Writing – review & editing, Methodology, Formal analysis, Data curation. **Daniel Urrutia-Cabrera:** Writing – review & editing, Resources, Methodology. **Jarmon G. Lees:** Writing – review & editing, Investigation, Formal analysis, Data curation. **Ren Jie Phang:** Writing – review & editing, Formal analysis, Data curation. **Geraldine M. Mitchell:** Writing – review & editing, Validation, Resources. **Raymond C.B. Wong:** Writing – review & editing, Validation, Supervision, Resources, Methodology. **Shiang Y. Lim:** Writing – review & editing, Writing – original draft, Validation, Supervision, Resources, Project administration, Methodology, Investigation, Funding acquisition, Formal analysis, Data curation, Conceptualization.

Funding and acknowledgement

Declaration of competing interest

The authors declare that they have no known competing financial interests or personal relationships that could have appeared to influence the work reported in this paper.

Appendix A. Supplementary data

Supplementary data to this article can be found online at https://doi.org/10.1016/j.bbrep.2024.101876.

References

[1] J. Folkman, M. Hochberg, Self-regulation of growth in three dimensions, J. Exp. Med. 138 (1973) 745–753, https://doi.org/10.1084/jem.138.4.745.

[2] S.V. Koduru, A.N. Leberfinger, D. Pasic, A. Forghani, S. Lince, D.J. Hayes, I.T. Ozbolat, D.J. Ravnic, Cellular based strategies for microvascular engineering, Stem Cell Rev Rep 15 (2019) 218–240, https://doi.org/10.1007/s12015-019-09877-4.

[3] M.A.C. Williams, D.B. Mair, W. Lee, E. Lee, D.H. Kim, Engineering three-dimensional vascularized cardiac tissues, Tissue Eng., Part B 28 (2022) 336–350, https://doi.org/10.1089/ten.TEB.2020.0343.

[4] S.Y. Lim, S.T. Hsiao, Z. Lokmic, P. Sivakumaran, G.J. Dusting, R.J. Dilley, Ischemic preconditioning promotes intrinsic vascularization and enhances survival of implanted cells in an in vivo tissue engineering model, Tissue Eng. 18 (2012) 2210–2219, https://doi.org/10.1089/ten.TEA.2011.0719.

[5] C.W. Chen, M. Corselli, B. Peault, J. Huard, Human blood-vessel-derived stem cells for tissue repair and regeneration, J. Biomed. Biotechnol. 2012 (2012) 597439, https://doi.org/10.1155/2012/597439.

[6] S.T. Hsiao, R.J. Dilley, G.J. Dusting, S.Y. Lim, Ischemic preconditioning for cell-based therapy and tissue engineering, Pharmacol. Ther. 142 (2014) 141–153, https://doi.org/10.1016/j.pharmthera.2013.12.002.

[7] H. Naito, T. Iba, N. Takakura, Mechanisms of new blood-vessel formation and proliferative heterogeneity of endothelial cells, Int. Immunol. 32 (2020) 295–305, https://doi.org/10.1093/intimm/dxaa008.

[8] D.M. Titmarsh, V. Nurcombe, C. Cheung, S.M. Cool, Vascular cells and tissue constructs derived from human pluripotent stem cells for toxicological screening, Stem Cell. Dev. 28 (2019) 1347–1364, https://doi.org/10.1089/scd.2018.0246.

[9] A.M. Kong, K.K. Yap, S.Y. Lim, D. Marre, A. Pebay, Y.W. Gerrand, J.G. Lees, J.A. Palmer, W.A. Morrison, G.M. Mitchell, Bio-engineering a tissue flap utilizing a

porous scaffold incorporating a human induced pluripotent stem cell-derived endothelial cell capillary network connected to a vascular pedicle, Acta Biomater. 94 (2019) 281–294, https://doi.org/10.1016/j.actbio.2019.05.067.

[10] S. Jang, A. Collin de l'Hortet, A. Soto-Gutierrez, Induced pluripotent stem cell-derived endothelial cells: overview, current advances, applications, and future directions, Am. J. Pathol. 189 (2019) 502–512, https://doi.org/10.1016/j.ajpath.2018.12.004.

[11] J.R. Bezenah, Y.P. Kong, A.J. Putnam, Evaluating the potential of endothelial cells derived from human induced pluripotent stem cells to form microvascular networks in 3D cultures, Sci. Rep. 8 (2018) 2671, https://doi.org/10.1038/s41598-018-20966-1.

[12] D. Hernandez, R. Millard, P. Sivakumaran, R.C. Wong, D.E. Crombie, A.W. Hewitt, H. Liang, S.S. Hung, A. Pebay, R.K. Shepherd, G.J. Dusting, S.Y. Lim, Electrical stimulation promotes cardiac differentiation of human induced pluripotent stem cells, Stem Cell. Int. (2016) 1718041, https://doi.org/10.1155/2016/1718041, 2016.

[13] K. Vlahos, K. Sourris, R. Mayberry, P. McDonald, F.F. Bruveris, J.V. Schiesser, K. Bozaoglu, P.J. Lockhart, E.G. Stanley, A.G. Elefanty, Generation of iPSC lines from peripheral blood mononuclear cells from 5 healthy adults, Stem Cell Res. 34 (2019) 101380, https://doi.org/10.1016/j.scr.2018.101380.

[14] T. Kao, T. Labonne, J.C. Niclis, R. Chaurasia, Z. Lokmic, E. Qian, F.F. Bruveris, S. E. Howden, A. Motazedian, J.V. Schiesser, M. Costa, K. Sourris, E. Ng, D. Anderson, A. Giudice, P. Farlie, M. Cheung, S.R. Lamande, A.J. Penington, C.L. Parish, L. H. Thomson, A. Rafii, D.A. Elliott, A.G. Elefanty, E.G. Stanley, GAPTrap: a simple expression system for pluripotent stem cells and their derivatives, Stem Cell Rep. 7 (2016) 518–526, https://doi.org/10.1016/j.stemcr.2016.07.015.

[15] C. Patsch, L. Challet-Meylan, E.C. Thoma, E. Urich, T. Heckel, J.F. O'Sullivan, S. J. Grainger, F.G. Kapp, L. Sun, K. Christensen, Y. Xia, M.H. Florido, W. He, W. Pan, M. Prummer, C.R. Warren, R. Jakob-Roetne, U. Certa, R. Jagasia, P.O. Freskgard, I. Adatto, D. Kling, P. Huang, L.I. Zon, E.L. Chaikof, R.E. Gerszten, M. Graf, R. Iacone, C.A. Cowan, Generation of vascular endothelial and smooth muscle cells from human pluripotent stem cells, Nat. Cell Biol. 17 (2015) 994–1003, https://doi.org/10.1038/ncb3205.

[16] L. Fang, S.S.C. Hung, J. Yek, L. El Wazan, T. Nguyen, S. Khan, S.Y. Lim, A. W. Hewitt, R.C.B. Wong, A simple cloning-free method to efficiently induce gene expression using CRISPR/Cas9, Mol. Ther. Nucleic Acids 14 (2019) 184–191, https://doi.org/10.1016/j.omtn.2018.11.008.

[17] G. Carpenter, S. Berndt, S. Ferratge, W. Rasband, M. Cuendet, G. Uzan, P. Albanese, Angiogenesis analyzer for ImageJ - a comparative morphometric analysis of "endothelial Tube Formation assay" and "fibrin bead assay", Sci. Rep. 10 (2020) 11568, https://doi.org/10.1038/s41598-020-67289-8.

[18] S.Y. Lim, D. Hernandez, G.J. Dusting, Growing vascularized heart tissue from stem cells, J. Cardiovasc. Pharmacol. 62 (2013) 122–129, https://doi.org/10.1097/FJC.0b013e31829372fc.

[19] C.P. Khoo, K. Micklem, S.M. Watt, A comparison of methods for quantifying angiogenesis in the Matrigel assay in vitro, Tissue Eng. C Methods 17 (2011) 895–906, https://doi.org/10.1089/ten.TEC.2011.0150.

[20] X. Fan, L. Cyganek, K. Nitschke, S. Uhlig, P. Nuhn, K. Bieback, D. Duerschmied, I. El-Battrawy, X. Zhou, I. Akin, Functional characterization of human induced pluripotent stem cell-derived endothelial cells, Int. J. Mol. Sci. 23 (2022), https://doi.org/10.3390/ijms23158507.

[21] M. Lindner, A. Laporte, L. Elomaa, C. Lee-Thedieck, R. Olmer, M. Weinhart, Flow-induced glycocalyx formation and cell alignment of HUVECs compared to iPSC-derived ECs for tissue engineering applications, Front. Cell Dev. Biol. 10 (2022) 953062, https://doi.org/10.3389/fcell.2022.953062.

[22] N.R. Ariyasinghe, R. de Souza Santos, A. Gross, A. Aghamaleky-Sarvestany, S. Kreimer, S. Escopete, S.J. Parker, D. Sareen, Proteomics of novel induced pluripotent stem cell-derived vascular endothelial cells reveal extensive similarity with an immortalized human endothelial cell line, Physiol. Genom. 55 (2023) 324–337, https://doi.org/10.1152/physiolgenomics.00166.2022.

[23] A. Pappalardo, L. Herron, D.E. Alvarez Cespedes, H.E. Abaci, Quantitative evaluation of human umbilical vein and induced pluripotent stem cell-derived endothelial cells as an alternative cell source to skin-specific endothelial cells in engineered skin grafts, Adv. Wound Care 10 (2021) 490–502, https://doi.org/10.1089/wound.2020.1163.

[24] W.J. Adams, Y. Zhang, J. Cloutier, P. Kuchimanchi, G. Newton, S. Sehrawat, W. C. Aird, T.N. Mayadas, F.W. Luscinskas, G. Garcia-Cardena, Functional vascular endothelium derived from human induced pluripotent stem cells, Stem Cell Rep. 1 (2013) 105–113, https://doi.org/10.1016/j.stemcr.2013.06.007.

[25] O.V. Halaidych, C. Freund, F. van den Hil, D.C.F. Salvatori, M. Riminucci, C. L. Mummery, V.V. Orlova, Inflammatory responses and barrier function of endothelial cells derived from human induced pluripotent stem cells, Stem Cell Rep. 10 (2018) 1642–1656, https://doi.org/10.1016/j.stemcr.2018.03.012.

[26] J.R. Bezenah, A.Y. Rioja, B. Juliar, N. Friend, A.J. Putnam, Assessing the ability of human endothelial cells derived from induced-pluripotent stem cells to form functional microvasculature in vivo, Biotechnol. Bioeng. 116 (2019) 415–426, https://doi.org/10.1002/bit.26860.

[27] A.M. Kong, S.Y. Lim, J.A. Palmer, A. Rixon, Y.W. Gerrand, K.K. Yap, W. A. Morrison, G.M. Mitchell, Engineering transplantable human lymphatic and blood capillary networks in a porous scaffold, J. Tissue Eng. 13 (2022) 20417314221140979, https://doi.org/10.1177/20417314221140979.

[28] J.M. Rutkowski, K.C. Boardman, M.A. Swartz, Characterization of lymphangiogenesis in a model of adult skin regeneration, Am. J. Physiol. Heart Circ. Physiol. 291 (2006) H1402–H1410, https://doi.org/10.1152/ajpheart.00038.2006.

[29] K. Shimamura, T. Nakatani, A. Ueda, J. Sugama, M. Okuwa, Relationship between lymphangiogenesis and exudates during the wound-healing process of mouse skin full-thickness wound, Wound Repair Regen. 17 (2009) 598–605, https://doi.org/10.1111/j.1524-475X.2009.00512.x.

[30] S.P. Herbert, D.Y. Stainier, Molecular control of endothelial cell behaviour during blood vessel morphogenesis, Nat. Rev. Mol. Cell Biol. 12 (2011) 551–564, https://doi.org/10.1038/nrm3176.

[31] V.V. Orlova, Y. Drabsch, C. Freund, S. Petrus-Reurer, F.E. van den Hil, S. Muenthaisong, P.T. Dijke, C.L. Mummery, Functionality of endothelial cells and pericytes from human pluripotent stem cells demonstrated in cultured vascular plexus and zebrafish xenografts, Arterioscler. Thromb. Vasc. Biol. 34 (2014) 177–186, https://doi.org/10.1161/ATVBAHA.113.302598.

[32] M.S. Collado, B.K. Cole, R.A. Figler, M. Lawson, D. Manka, M.B. Simmers, S. Hoang, F. Serrano, B.R. Blackman, S. Sinha, B.R. Wamhoff, Exposure of induced pluripotent stem cell-derived vascular endothelial and smooth muscle cells in coculture to hemodynamics induces primary vascular cell-like phenotypes, Stem Cells Transl Med 6 (2017) 1673–1683, https://doi.org/10.1002/sctm.17-0004.

[33] L. Atchison, H. Zhang, K. Cao, G.A. Truskey, A tissue engineered blood vessel model of hutchinson-gilford progeria syndrome using human iPSC-derived smooth muscle cells, Sci. Rep. 7 (2017) 8168, https://doi.org/10.1038/s41598-017-08632-4.

[34] R.A. Wimmer, A. Leopoldi, M. Aichinger, N. Wick, B. Hantusch, M. Novatchkova, J. Taubenschmid, M. Hammerle, C. Esk, J.A. Bagley, D. Lindenhofer, G. Chen, M. Boehm, C.A. Agu, F. Yang, B. Fu, J. Zuber, J.A. Knoblich, D. Kerjaschki, J. M. Penninger, Human blood vessel organoids as a model of diabetic vasculopathy, Nature 565 (2019) 505–510, https://doi.org/10.1038/s41586-018-0858-8.

[35] A. Papapetropoulos, G. Garcia-Cardena, J.A. Madri, W.C. Sessa, Nitric oxide production contributes to the angiogenic properties of vascular endothelial growth factor in human endothelial cells, J. Clin. Invest. 100 (1997) 3131–3139, https://doi.org/10.1172/JCI119868.

[36] S. Babaei, D.J. Stewart, Overexpression of endothelial NO synthase induces angiogenesis in a co-culture model, Cardiovasc. Res. 55 (2002) 190–200, https://doi.org/10.1016/s0008-6363(02)00287-0.

[37] C. Heiss, A. Rodriguez-Mateos, M. Kelm, Central role of eNOS in the maintenance of endothelial homeostasis, Antioxidants Redox Signal. 22 (2015) 1230–1242, https://doi.org/10.1089/ars.2014.6158.

[38] D. Fukumura, T. Gohongi, A. Kadambi, Y. Izumi, J. Ang, C.O. Yun, D.G. Buerk, P. L. Huang, R.K. Jain, Predominant role of endothelial nitric oxide synthase in vascular endothelial growth factor-induced angiogenesis and vascular permeability, Proc. Natl. Acad. Sci. U. S. A. 98 (2001) 2604–2609, https://doi.org/10.1073/pnas.041359198.

[39] J. Granton, D. Langleben, M.B. Kutryk, N. Camack, J. Galipeau, D.W. Courtman, D. J. Stewart, Endothelial NO-synthase gene-enhanced progenitor cell therapy for pulmonary arterial hypertension: the PHACeT trial, Circ. Res. 117 (2015) 645–654, https://doi.org/10.1161/CIRCRESAHA.114.305951.

[40] F. Leo, T. Suvorava, S.K. Heuser, J. Li, A. LoBue, F. Barbarino, E. Piragine, R. Schneckmann, B. Hutzler, M.E. Good, B.O. Fernandez, L. Vornholz, S. Rogers, A. Doctor, M. Grandoch, J. Stegbauer, E. Weitzberg, M. Feelisch, J.O. Lundberg, B. E. Isakson, M. Kelm, M.M. Cortese-Krott, Red blood cell and endothelial eNOS independently regulate circulating nitric oxide metabolites and blood pressure, Circulation 144 (2021) 870–889, https://doi.org/10.1161/CIRCULATIONAHA.120.049606.